CHAPTER -07

SAFETY ANALYSIS AND RESEARCH

SAFETY ANALYSIS AND RESEARCH

AERB recognizes the importance of Safety Analysis & Research in support of its regulatory functions. In-house safety related R&D helps in obtaining deeper insights into the issues concerning nuclear and radiation safety to arrive at technically sound regulatory decisions. Safety analysis and research activities are carried out by AERB as a part of its regulatory activities. Brief overview of several important developmental studies taken up by AERB during this year is presented in the following sections.

7.1 Reactor Thermal Hydraulics Safety Studies

7.1.1 Studies on Sodium Aerosol Characteristics in SFR Cover Gas Region

In Sodium-cooled Fast Reactors (SFR), due to the reactive nature of sodium, provision of an inert isolation layer (known as cover gas space) is provided above the primary sodium boundary. During reactor operation, sodium aerosols are generated continuously via sodium evaporation and transported to the cover gas space. Understanding the evolution and transport of sodium aerosols within the cover gas is of paramount importance for comprehending their dynamics under various reactor-operating conditions. A detailed CFD model of the cover gas geometry of SILVERINA facility available at IGCAR was developed in Open FOAM framework. This study was useful for validation of the numerical model and subsequently for development of a correlation to predict the aerosol mass concentration as a function of temperature difference between roof slab and sodium pool. The present model can be used to obtain inputs for radiological impact assessment. The variation of aerosol mass concentration in the cover gas region is shown in Fig. 7.1.1 (a) and (b).

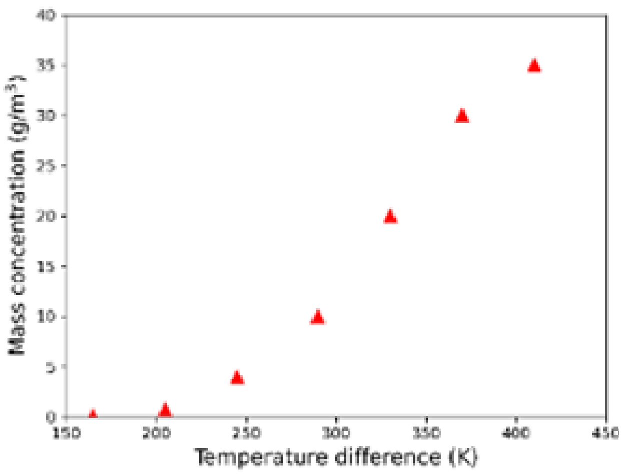

Fig. 7.1.1 (a) Mass Concentration vs. Temperature Difference between Roof-Slab Bottom Plate Temperature and Sodium Tool Temperature

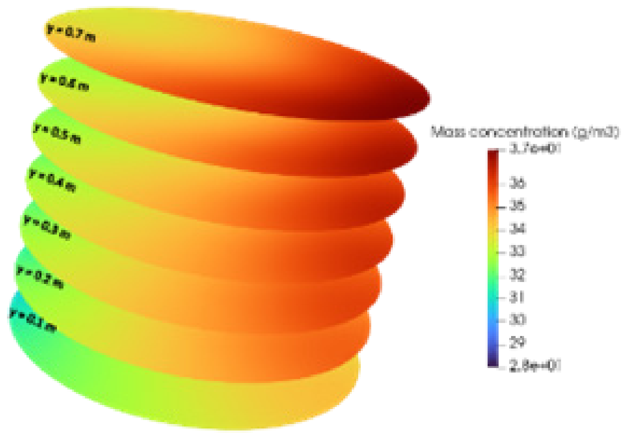

Fig. 7.1.1 (b) Mass Concentration Variation along Height for Operating Conditions (Pool Temperature: 823 K and Roof Temperature: 413 K)

7.1.2 CFD Simulation of Temperature Distribution in KAPP 3 Containment

The objective of this study was to calculate the overall heat/temperature distribution inside 700 MWe PHWR containment due to the heat released from Feeder Header Insulation Cabinet (FHIC) and other sources and to assess the efficacy of the ventilation system. For a given ventilation system configuration in 700 MWe PHWR containment, a model has been developed in CFD code. The detailed configuration of FHIC, coolers, fans and insulation system has been considered in model. For 50% power case and given cooler and fan capacity, CFD simulation was performed to estimate the containment temperature distribution and results were compared with the measured plant data. It was observed that CFD model is closely matching the actual temperature in the containment with the given heat loss conditions. The temperature distribution in the containment for the FM vault plane is shown in Fig.7.1.2. It shows the different high temperature zone as well as effect of the ventilation system on temperature distribution.

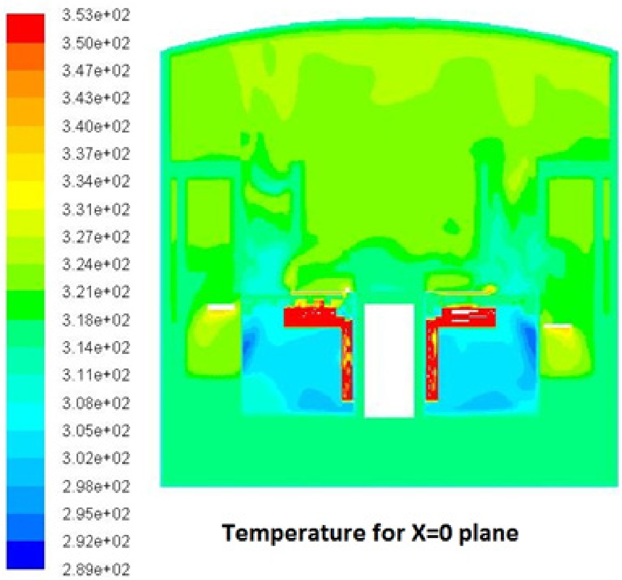

Fig.7.1.2: Temperature Distribution FM Vault Plane

7.2 Severe Accident Studies

7.2.1 Critical Heat Flux on PHWR Calandria during Severe Accident

A comprehensive hydrodynamics model based on two-phase boundary layer flow was developed to obtain critical heat flux (CHF) on calandria outer surface. The objective was to assess the thermal margin available for success of In-Vessel Retention (IVR) strategy, which is considered to be a key severe accident management option in PHWRs. The model was benchmarked using experimental data from three facilities, namely ULPU-III, SBLB and BARC facility for curved section of PHWR calandria vessel reported in literature. It was then applied for estimating CHF on PHWR-700 calandria vessel outer surface for a scenario involving LOCA followed by loss of all heat sinks. Similar studies were undertaken for PHWR-220 calandria vessel. Several parametric studies were also conducted to bring out the effect of vessel size, system pressure, sub-cooling of vault water and depth of submergence of vessel on CHF. The model was then applied to estimate CHF on PHWR-700 calandria tube outer surface under the same accident condition.

7.2.2 Numerical Studies on In-Vessel Corium Retention in PHWR-700 during Severe Accident Conditions

A numerical model is developed using Open FOAM CFD software to study the core melting and solidification process in the calandria vessel following a postulated severe accident scenario. The model uses finite volume method for obtaining the solution. Convection and radiation boundary conditions are applied on the top of corium region. On the vessel bottom, suitable boiling heat transfer correlations are used to capture the crust formation. Heat transfer to inner surface of calandria vessel is analysed in detail.

Fig. 7.2.2 (a) shows the temperature distribution in corium melt pool and calandria vessel under steady state conditions. Velocity distribution in the molten region of the pool is shown in Fig. 7.2.2 (b). This study has provided additional inputs for assessing the thermal margin available for in-vessel retention (IVR) in calandria.

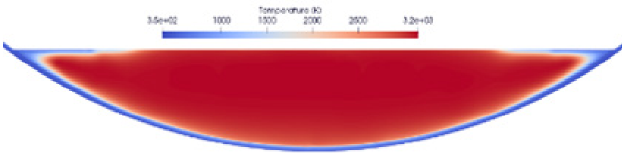

Fig. 7.2.2 (a) Temperature Distribution in Corium Melt Pool and Calandria Vessel

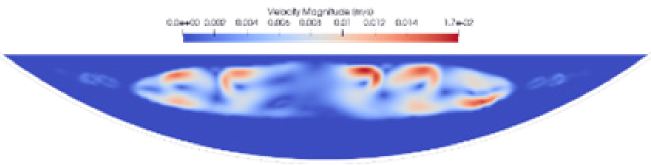

Fig. 7.2.2 (b) Velocity Distribution in the Molten Region of Pool

7.2.3 Analysis of Extended Station Blackout Scenario in Spent Fuel Pool of PHWRs

In a PHWR, spent fuel bundles are stored underwater in trays that are stacked in the form of racks. The spent fuel pool water removes decay heat and provides shielding against radiation. The capability of PHWR spent fuel pool (SFP) for heat removal was assessed for an extended station blackout scenario without considering any mitigating actions. It was assumed that the SFP is loaded to the maximum extent, with spent fuel discharged over a period of 10 years together with one full core unload. As per analysis, the time available for preventing thermal transient and chemical oxidation in fuel bundles is around 10 days. The results compare well with utility submission on evaporation rate and fall in water level.

7.2.4 Transients under Non-availability of One or More PDHRS Banks

The effect of non-availability of one or more PDHRS, of PHWR-700MWe, during a Station Blackout (SBO) event was investigated using RELAP5/Mod 3.4. Failures of one PDHRS in one loop and failure of one PDHRS in each of the loops were considered, with different valve-in times, to examine their influence on thermal-hydraulic transients. It was found that oscillations in the primary loop were effectively mitigated when there was a simultaneous failure of one PDHRS in both the loops. This was in contrast to oscillations

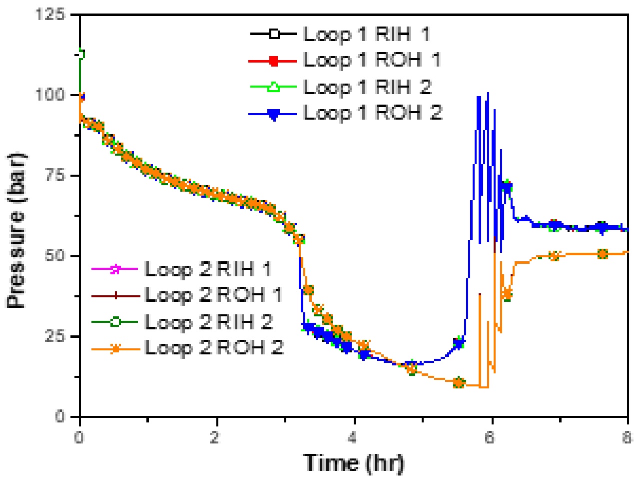

(a) Failure of one PDHRS in one Loop

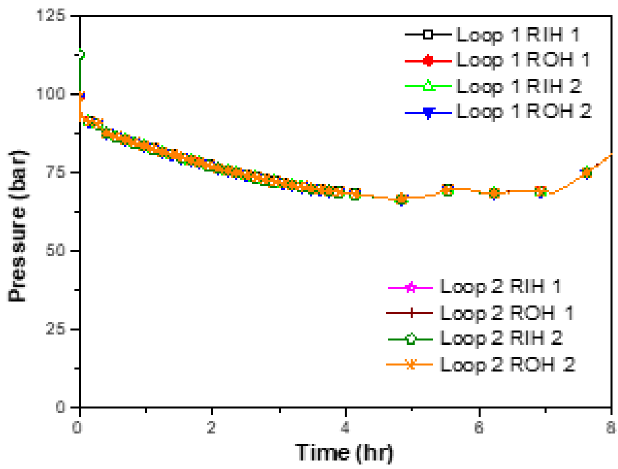

(b) Failure of two PDHRS, one in each Loop

Fig. 7.2.4: Variation of PHT Header Pressure

observed in the case of failure of one PDHRS in a single loop. The symmetrical operation during simultaneous failure of two PDHRS appears to prevent instabilities and flow reversals during the transient phase. Fig. 7.2.4 depicts the variation in PHT pressure.

7.2.5 Disassembly Phase Analysis for a Medium Sized MOX Fuelled SFR

A coupled neutronics-hydrodynamics compute code is developed to model the super-prompt critical power excursion during disassembly phase of Core Disruptive Accident (CDA) in a fast reactor. This computer code has been developed to provide an estimate of the thermal energy released and work potential during the disassembly phase of CDA in a medium sized MOX fuelled Sodium Cooled Fast Reactor (SFR). The code is validated against a severe transient event in the Fast Flux Test Facility (FFTF) reactor. It is then applied to study disassembly phase in a typical medium sized MOX fuelled SFR . Fig. 7.2.5 (a) and (b) show the evolution of thermal power and energy for voided and non-voided core states respectively. Termination of the transient occurs early in the case of non-voided core due to faster rate of negative reactivity insertion. The code has capability to predict peak pressure, thermal energy and the work potential for the disassembly phase.

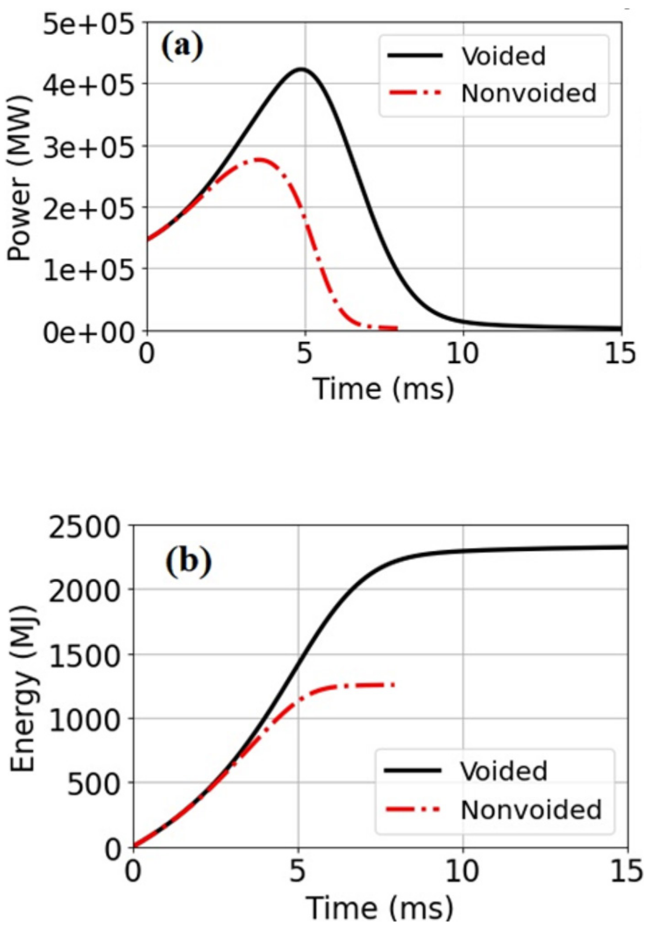

Fig.7.2.5: Variation of (a) Power and (b) Energy during Disassembly Phase in a Medium sized MOX Fuelled SFR for fully Sodium Voided and Non-voided Core States

7.3 Safety Analysis Code Development & Benchmarking

7.3.1 Analysis of End Fitting Failure Event during Fuel Handing Operation in PHWRs

A fuel handling accident condition is postulated in which the fuelling machine disengages without the seal plug being properly fixed on the coolant channel resulting in ejection of all the 12 fuel bundles from the coolant channel on the FM vault floor. These bundles generate decay heat as per their operating history but experience loss of cooling resulting in increase in temperature. This event was analysed in detail using in-house developed computer program called SAAP. The fuel bundle initial temperature corresponds to full power operating conditions for the highest rated channel. Heat loss by radiation and natural convection are considered. Numerical studies have shown that 8 out of 12 fuel bundles could experience high temperature transients and clad failure. The maximum clad temperature reached is around 1500°C for the central pin of highest rated bundle as shown in Fig.7.3.1. Under

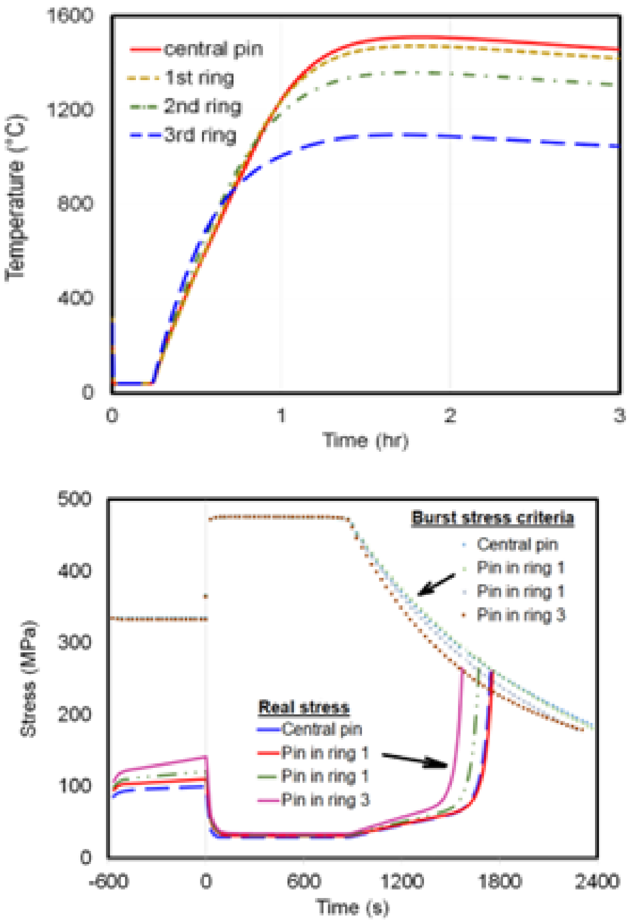

Fig. 7.3.1: Temperature Transients in Fuel Pin and failure by Burst Stress Criteria for the Highest Rated Fuel Bundle

unlimited steam condition, around 720g of H_2 is generated from all the ejected fuel bundles.

7.3.2 Thermal Qualification of Type B (U) Cask

Numerical techniques required for thermal qualification of radioactive material transport cask to satisfy regulatory requirements has been shown by a detailed study. A typical type B(U) fuel bundle cask was selected for analysis. Type B(U) casks contain materials with reasonably high levels of radioactivity, such as spent fuel, high concentration of certain radioisotopes such as ^{137}Cs, cobalt sources etc. The focus of this study was to (a) outline the methods needed to capture melting and solidification of shielding lead during fire and post fire transients and (b)

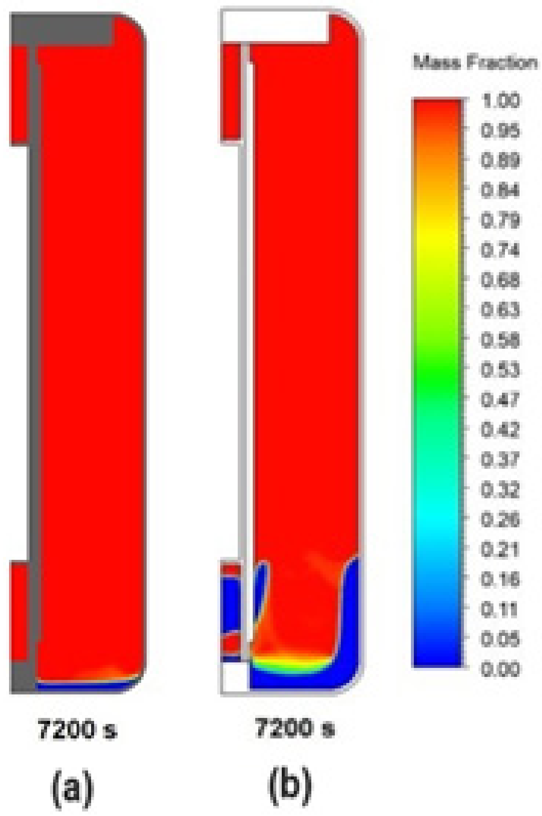

Fig.7.3.2: Commencement of Solidification at the bottom of the Cask; (a) Hydrocarbon-air Curve, (b) Constant 800°C Fire

bring out the role played by choice of fire curve and cask surface boundary conditions on the transients. The study covers simulation of normal transport conditions, followed by fire and post-fire transient analysis. Initial temperature of cask is taken same as ambient temperature. Half an hour fire exposure conditions were simulated using boundary conditions in the form of hydrocarbon fuel-air fire, ISO-834 curve as well as considering constant 800°C surrounding temperature. During the hydrocarbon fuel-air fire test, lead is found to melt before the completion of the test whereas for the 800°C case, only 69.7% of lead had melted. Solidification process begins at the bottom of the cask during cool-down phase. Solidification begins earlier for the constant 800°C case. Fig.7.3.2 show contour plots of solidified lead for two cases. This study is intended to provide a benchmark against which regulatory review of submissions made by the utilities can be conducted.

7.3.3 Upgradation of the In-house Code Severe Accident Analysis Program (SAAP)

The in-house developed Severe Accident Analysis program (SAAP) has been developed to study DEC conditions such as LOCA and failure of ECCS and station blackout in all Indian PHWRs. This code has been upgraded by undertaking the development of a fuel pin model that simulates thermal and mechanical behaviour of the PHWR fuel pin under accident conditions. The model incorporates one dimensional heat transfer equation in cylindrical coordinate system with constitutive relations for thermo-physical properties, fission gas generation and release, pellet-clad gap conductance, pin internal pressure, circumferential stress, and burst criteria, zircaloy oxidation and hydrogen generation. This model is used to develop a PHWR fuel bundle model by incorporating detailed convection and radiation heat transfer models. The models are benchmarked and incorporated into the basic structure of SAAP code as shown in Fig. 7.3.3.

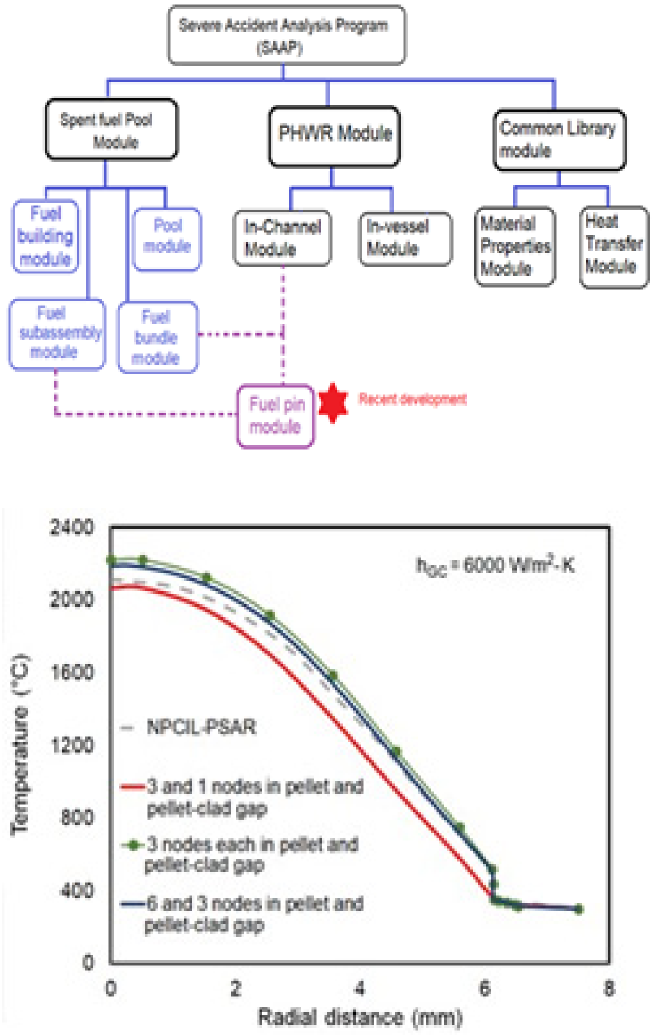

Fig. 7.3.3: Development of Fuel Pin Model within the SAAP Code and Benchmarking for Operating Parameters of PHWR

7.3.4 Studies on Transients of Coupled Natural Circulation Loops with Application to PDHRS

A generalized coupled loop two-phase computer code based on drift flux model is developed for application to passive reactor core cooling systems. It can simulate various orientations of heater-cooler in both loops. It employs water-steam property subroutine instead of the Boussinesq approximation. A key feature available in this code is its ability to capture flashing phenomena in the vertically oriented pipes. The code is validated against experimental data from several facilities such as CIRCUS-IV, PMCS and VISTA. A typical start-up flow transient in primary and secondary loop is depicted in Fig 7.3.4. The code can capture single-phase natural circulation stage (SNS), intermittent or transition stage (ITS) as well as the two-phase natural circulation stage (TNS). The influence of geometrical and operating parameters is also investigated and a sensitivity analysis has been carried out to identify dominant variables affecting the transients. This model can now be applied to study performance of PDHRS of PHWR-700 and passive moderator cooling system in AHWR.

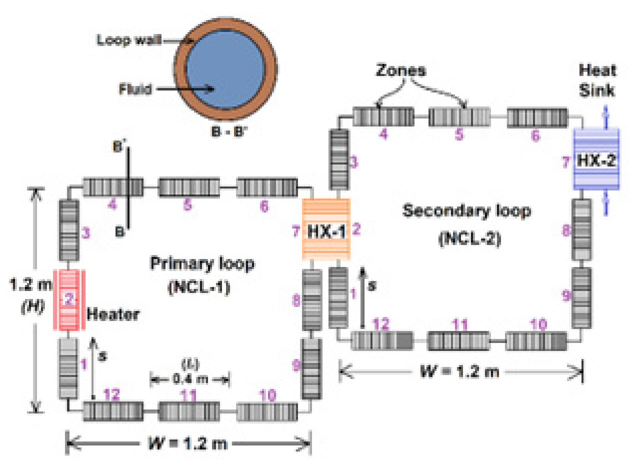

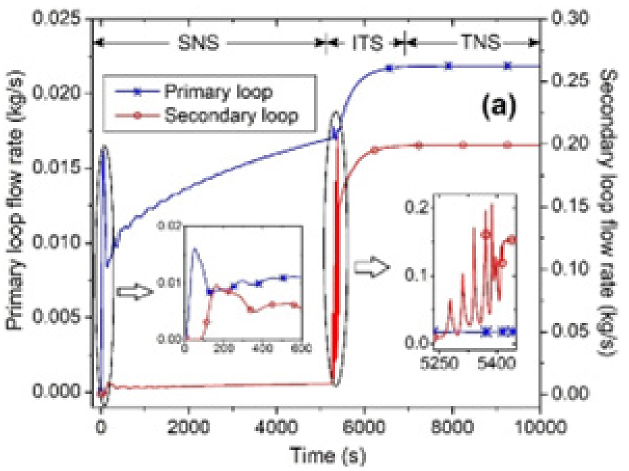

Fig. 7.3.4: Vertically Coupled NCLs and a Typical Flow Transient

7.3.5 Numerical Modelling of Fire Development in the Cable Spreader Room of an NPP

A mathematical model for cable fire development in a room containing several vertical vents (windows) is developed. The mass, energy and oxygen conservation equations are derived from basic principles and solved simultaneously to obtain fire parameters in the room. The model is benchmarked against Hinsdale Telephone Exchange (HTE), Illinois, USA fire data. It is then applied to study the consequence of cable fire in the cable spreader room of an NPP. The various processes occurring in the room during fire development such as; heat release rate, mass burning rate, pressure and temperature rise, breakage of window glass panes, inflow and out flow of air and hot gases, temperature profile across boundaries are captured. This model differs from earlier works by prescribing a criterion to arrive at a realistic, steady cable insulation-burning phase following the initial fast growth phase. The sudden opening of windows due to breakage of glass panes is also modelled. Fig. 7.3.5 shows the geometry of typical cable spreader room and cable burning transient.

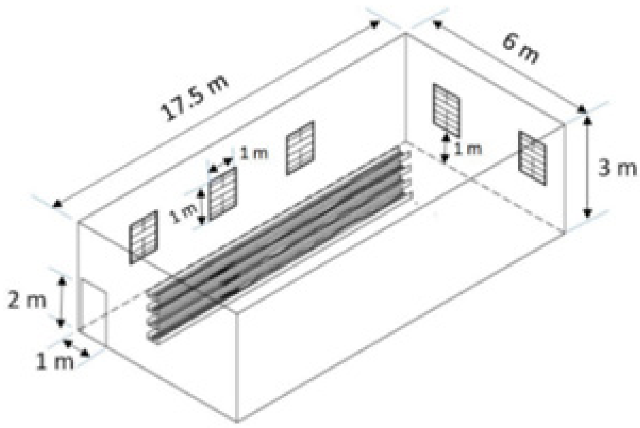

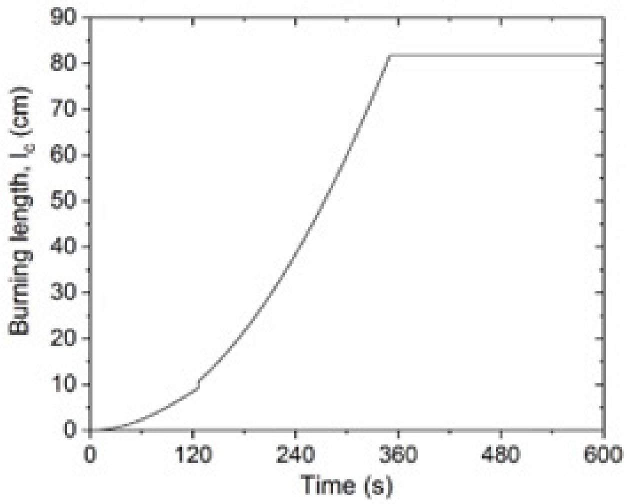

Fig. 7.3.5: Schematic of Cable Spreader Room and Cable Burning Transient

7.3.6 Contribution to PRABHAVINI Code Assessment

PRABHAVINI is an integral safety analysis code that is being developed by BARC along with other DAE units and AERB to analyze accident conditions in nuclear reactors. AERB is participating in development and validation of various modules of PRABHAVINI. As a part of PRABHAVINI Code assessment following activities were carried out:

a) Development of 700 MWe PHWR Containment Model in PRABHAVINI

Earlier, PARIRODHAN, a containment thermal hydraulic module of PRABHAVINI v3.0 was assessed against NUPEC M-4-3 hydrogen/ helium distribution test. For subsequent use of PRABHAVINI for NPPs, development of 700 MWe PHWR containment model in PRABHAVINI was taken up. 700 MWe PHWR primary containment is modelled using several compartments. Opening between compartments are modelled using junctions while thermal inertia of containment walls and internal structures are modelled using SWALL (heat structures) components. The input deck was verified. To further gain confidence of correctness of 700 MWe PHWR containment input deck of PRABHAVINI, containment peak pressure (Fig. 7.3.6(a)) and temperature during LB-LOCA was estimated and compared with utility's predictions and found to be reasonably matching.

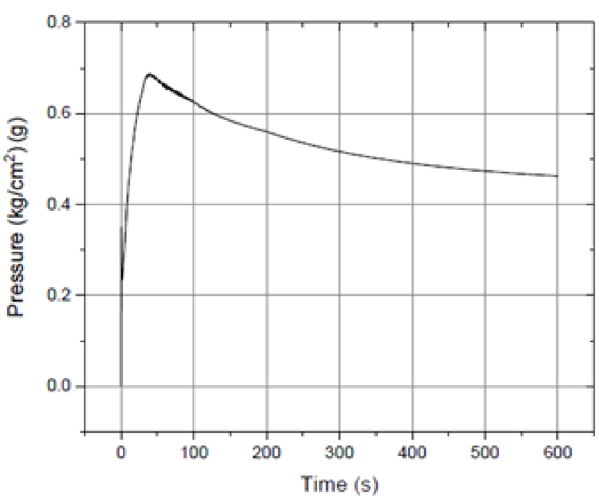

Fig. 7.3.6(a): Containment Pressure Predicted by PRABHAVINI

b) Assessment of PRAVAH and ABHA Module of PRABHAVINI

As part of an independent assessment and user feedback exercise for the PRABHAVINI code, an evaluation of the PRAVAH module (a computational model for simulating the heat transport system) and the ABHA module (a computational model for simulating the reactor core and its components) against the RELAP5 code has been conducted. One pass of 540 MWe PHWRs from Reactor Inlet Header (RIH) to Reactor Outlet Header (ROH) was modelled with one hot channel and one single average channel. Subsequently, a pseudo transient simulating a steady pressure change in the hot channel from an initial pressure of 11.4 MPa to 10.4 MPa followed by a return to 11.4 MPa was imposed. The resulting change in mass flow rate in the hot channel (Fig. 7.3.6(b)), change in total power (due to reactivity feedback) (Fig 7.3.6(c)), void fraction

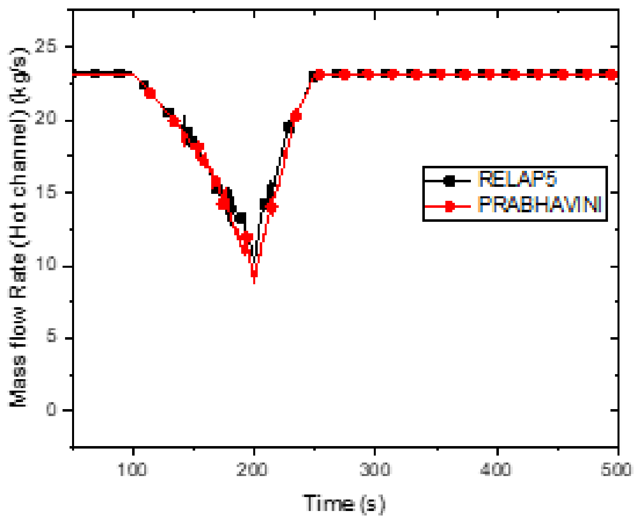

Fig. 7.3.6(b): Variation in Mass Flow Rate in Hot Channel

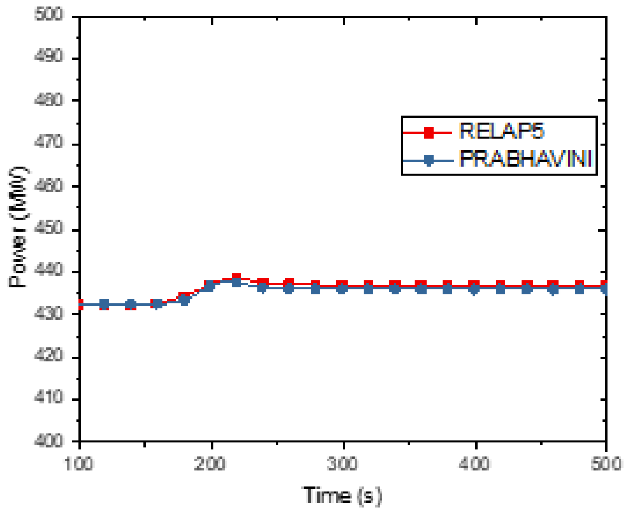

Fig. 7.3.6(c): Reactor Power

in both hot and average channel and core exit temperature was compared and found to be in good agreement.

c) Steady State Analysis for 540 MWe PHWR using PRABHAVINI

As part of the ongoing assessment of the PRABHAVINI code and to provide user feedback to the developers, a steady-state analysis of a 540 MWe PHWR has been undertaken.

In the modelling process, the reactor channel was represented using the CPIPE component, with one pass simulated using two CPIPE components. One component represents the highest power channel, and the other represents average channel. The remaining three passes were modelled using three separate CPIPE components. Various core components, including Fuel, PT & CT, and associated radiation heat transfer, were also modelled using various RCOMP component of ABHA module. The simulation of reactor power was achieved using the NEUPOW component of the ABHA module. The secondary system modelling included the representation of the Steam Generator (SG) with feed water flow and steam flow as boundaries. Additionally, the Pressurizer, PHT pressure control logic, and SG level control were also included in the model. The steady-state values of crucial parameters, such as reactor power, header pressure & temperature, SG pressure and temperature, core exit temperature, and channel mass flow rate, were found to be within 1% of nominal values. The variations in reactor power and mass flow rate are illustrated in Fig. 7.3.6 (d) & (e), respectively.

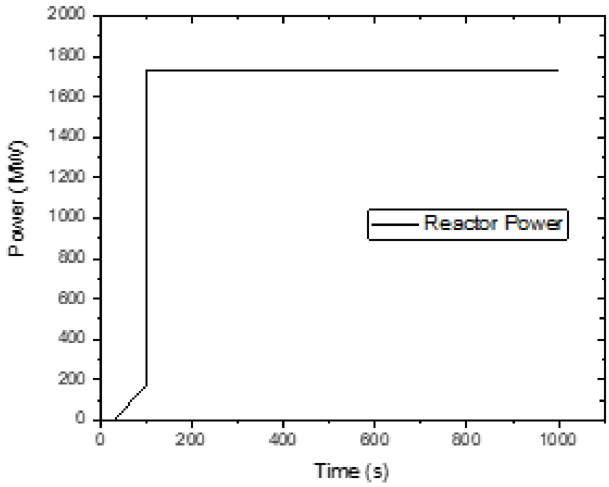

(d) Reactor Power

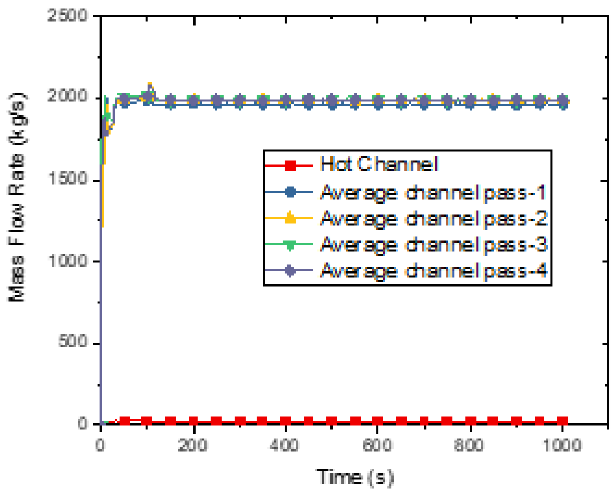

(e) Variation in Mass Flow Rate in Hot Channel

Fig.7.3.6: Steady State Analysis of 540 MWe PHWRs

7.3.7 Coupled Thermal-Hydraulics Neutron Kinetics Benchmark Exercise

AERB participated in the Phase 1A (steady and transient neutronics) of benchmark exercise ABCS initiated by AERB using the in-house developed multi-point kinetics code MPKC. The MPKC code was developed primarily to couple neutronics with system thermal hydraulic code RELAP5. The Multi-point kinetics formulation is based on dividing the entire core into several regions and solving coupled ordinary differential equations (ODEs) describing kinetics in each region. The capability of this code was demonstrated by validating against the AECL 7236 benchmark problem describing a hypothetical LOCA arrested by SCRAM in a PHWR for large reactivity insertion rates. The MPKC code has been utilized to simulate ABCS Phase 1A benchmark problem. Effective multiplication factors (K_{eff}) for different core configurations, normalized azimuthal power distribution for steady state configuration, normalized total power and 3D peaking factor as desired by the benchmark have been estimated with SCRAM of 26 SORs for half-core voiding transients. The estimated results are in close agreement with the reference results of the benchmark. Salient results are provided in Fig. 7.3.7(a), 7.3.7(b), 7.3.7(c) and 7.3.7(d) respectively for steady state normalized power distribution, normalized power distribution during half core voiding transient and 3D peaking factor during half core voiding transient.

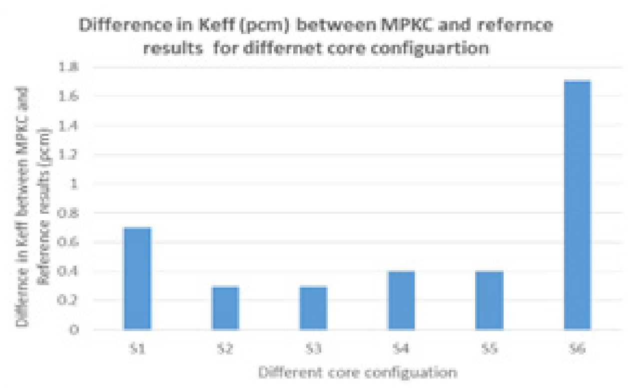

Fig. 7.3.7(a): K_{eff} Comparison for Different Cases

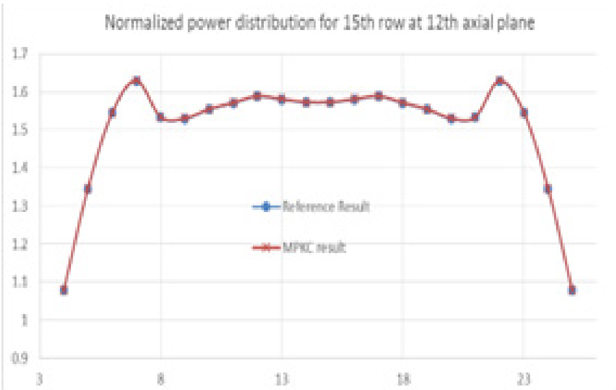

Fig. 7.3.7(b): Steady State Normalized Power Distribution Comparison

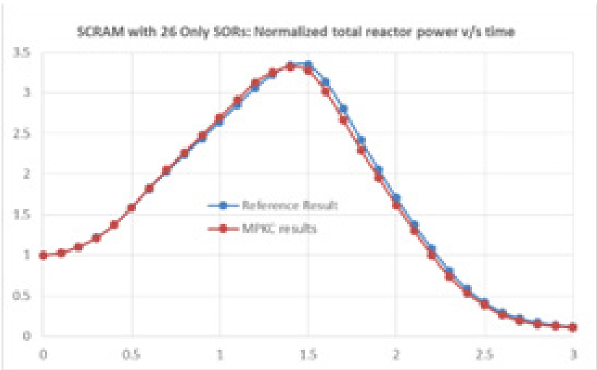

Fig. 7.3.7(c): Normalised Power Distribution Comparison during Half Core Voiding Transient

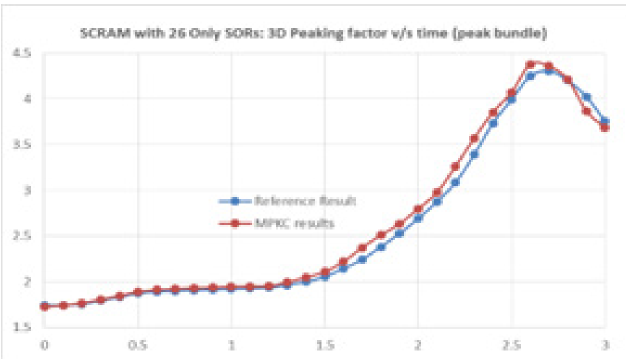

Fig. 7.3.7(d): 3D Peaking Factor Comparison during Half Core Voiding Transient

7.3.8 Development of Reactor Dynamics Code REDAC at AERB

Safety analysis of a nuclear reactor requires estimation of neutron flux, power distribution and associated core thermal state during normal operation and postulated events. A transient 3D reactor kinetics code REDAC (REactor Dynamics Analysis Code) has been developed at AERB for this purpose over the past few years. It solves 3D multi-group neutron diffusion equation, coupled with the fuel-coolant heat transport equations. REDAC offers flexibility in terms of reactor geometry, boundary conditions, spatial discretization and solution methods. Efficient numerical schemes have been employed for solving the governing equations. The performance of REDAC has been demonstrated by solving a few benchmark problems in different types of reactors. Some of these benchmarks include AECL-7236 (PHWR), AER FCM-101, AER DYN-001, AER DYN-002 (VVERs) and IAEA benchmark problems on PWRs. REDAC has also provided valuable inputs for safety analysis of Indian reactors. Some of the safety analyses performed using REDAC include estimation of critical channel powers for 700 MWe IPHWR, simulation of low power physics experiments in 1000 MWe VVER, simulation of power transients associated with LOCA and LORA in IPHWRs, etc. REDAC has a broad spectrum of applicability in terms of reactor geometry and the nature of the static/transient problems to be analysed. For illustration, Fig. 7.3.8 shows REDAC results for a couple of benchmark problems.

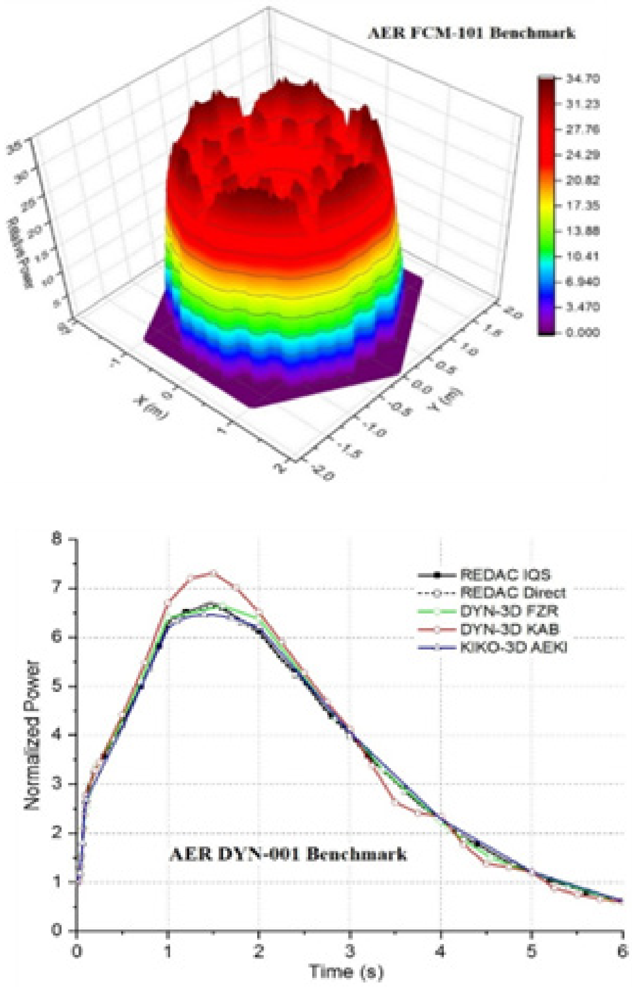

Fig. 7.3.8: Power Distribution (AER FCM-101 Benchmark) and Power History (AER DYN-001 Benchmark) Calculated using REDAC

7.4 Radiological Impact Assessment Studies

7.4.1 Determination of Source Term for Radioactive Releases by Inverse Modelling Technique

Assessment of the radionuclide source term and its composition is of vital importance in the event of any nuclear accident. Inverse modelling methods that combine environmental measurements with suitable atmospheric dispersion models are one of the effective methods for the estimation of the source term. In the present study, a variation approach that directly makes use of the gamma dose rate measurements for the source term estimation is used for a hypothetical release of radionuclides from Tarapur NPP site as a sample case. This modelling methodology is able to reconstruct the time evolution of the radionuclide species emitted for the fictitious release considered

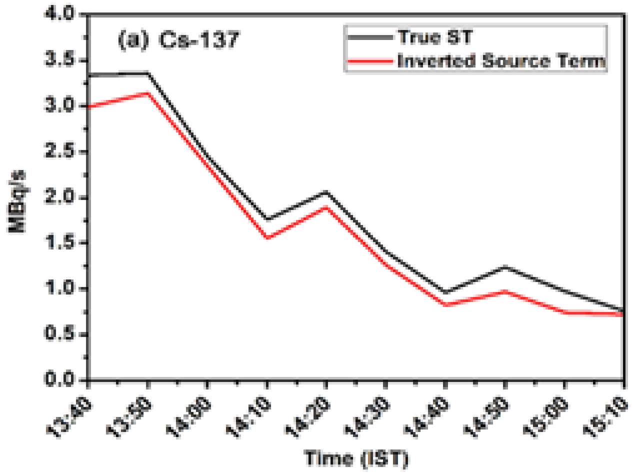

Fig. 7.4.1: Comparison of Inverted and True Source Term of ^{137}Cs

in the study. The study brought out that the estimated source term is in reasonably good agreement with the observed values in 90% of cases analysed. As a sample case, the comparison of the inverted and true source term of ^{137}Cs is shown in Fig. 7.4.1. The study also demonstrates the possible use of variational approach based inverse modelling technique in future Decision Support Systems for estimation of radioactive source term during nuclear emergencies.

7.5 Experimental Studies

7.5.1 Turbine Lube Oil Pool Fire Tests in Compartment Fire Test Facility (CFTF)

SRI-AERB has commissioned a Compartment Fire Test Facility (CFTF) for fire safety research in the area of pool & cable fires and its impact on safety. Confirmatory testing of burning behaviour of combustible fuels & solvents used in NPPs is undertaken in this facility. As part of this activity, a small setup was designed to test turbine lube oil used in PFBR to assess its fire hazard potential. Several pool fire tests were conducted to assess its burning behaviour. Since the lube oil is classified as a class-III liquid that is difficult to ignite, different ignition methods involving

Fig 7.5.1: Pool Fire Experimental Facility for PFBR Turbine Oil

supply of electrical and thermal energy were employed to study its ignitability. Fig. 7.5.1 shows one experimental campaign in progress.

7.5.2 Influence of Catalyst Dosage on the Uptake of Uranium

The study was taken up to find out a solution for the uptake of uranium for very lean uranium sources like tailing ponds, rain water discharged from flooded uranium mines etc. As the technology adopted would find a solution for minimizing the uranium discharge to the environment, it would help in future regulatory decision making. As a

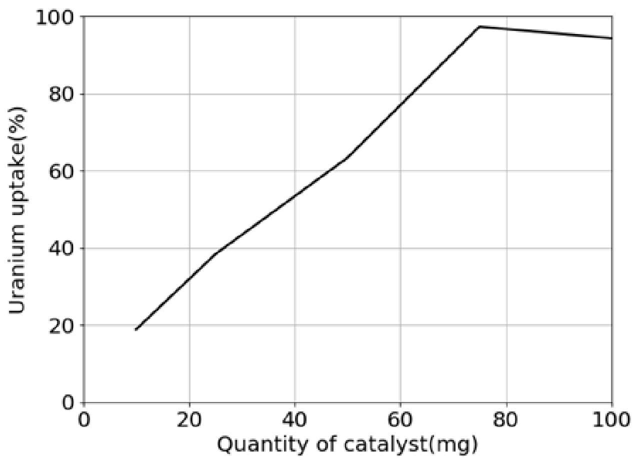

Fig.7.5.2: Influence of Catalyst Dosage on the Uptake of Uranium

part of the study, Graphene Oxide-Chitosan (CTS-GO) composite was synthesized in-house by cross linking chitosan and graphene oxide using modified Hummer's method.

The synthesized composite was characterized using XRD and SEM to assess its structure and morphology. Uranium adsorption studies indicate that more than 97% of uranium in uranyl nitrate solution could be removed at pH 4. The influence of pH towards the removal of uranium was found to follow the order acidic < neutral< alkaline indicating the electrostatic interaction between the catalyst and uranium at lower pH ranges although significant removal was observed in all the pH ranges. Results of this study shows that the synthesized chitosan-graphene oxide composite can effectively remove uranium from effluents arising from different process streams (Fig. 7.5.2).

7.5.3 Studies on Sorption of Iodine Species using Silver-doped Alumina

The study aims in keeping the iodine species in the aqueous phase itself without making it airborne thereby minimizing the release to the gaseous phase and hence to the environment. For reducing the volatile iodine inside reactor containment, it is essential to devise methodologies to retain iodine species in the sump without making it airborne, thereby limiting its potential transport out of the containment. Towards this study, silver

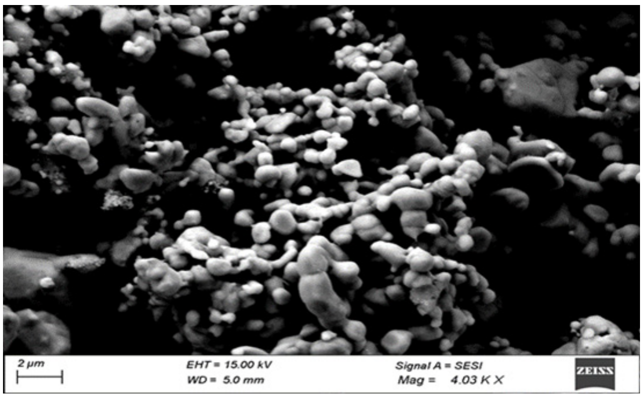

Fig.7.5.3(a): SEM Image of Silver Coated Alumina

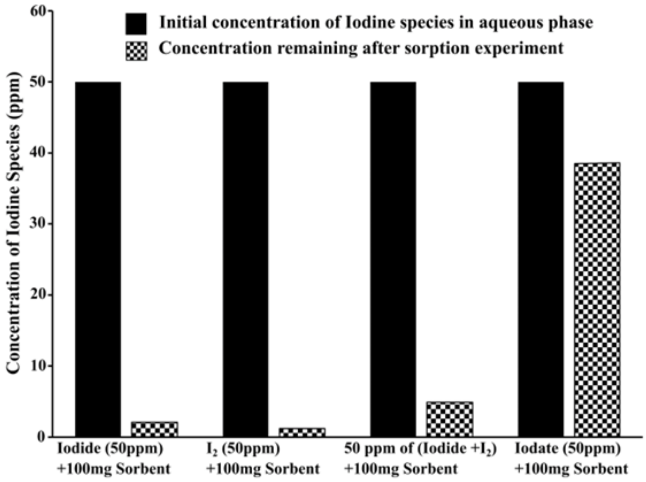

Fig.7.5.3(b): Sorption of Iodine Species using Silver-coated Alumina

coated alumina was synthesized in-house by chemical impregnation method (Fig. 7.5.3(a)). For the iodine sorption experiments, simulated sump solutions containing 50mg/L of iodine species were equilibrated with 100mg of catalyst for 2 hours and the extent of iodine retention was estimated using ion chromatographic method. More than 95% of iodine species and 23% of iodate could be retained by the catalyst (Fig. 7.5. 3(b)). The study demonstrates that the synthesized silver coated alumina catalyst is highly effective for the retention of iodine species, which could retain them in the aqueous phase itself.

7.5.4 Theoretical and Experimental Studies to investigate the Behaviour of Iodine inside Reactor Containment under Postulated Accidental Conditions

Theoretical studies were carried out using the FACTSAGE software based on chemical thermodynamics to predict the possible reaction products of iodine interaction with various species in the gaseous and aqueous phase. In parallel, experimental studies were carried out at the Chemistry laboratory of SRI using an iodine experimental set up to understand the influence of pH, temperature, organic impurities, iodinepaint interaction and irradiation effects on the iodine behaviour viz. transport and speciation. Both theoretical and experimental studies reveal that the rate of formation of methyl iodide formed upon iodine interaction with painted surfaces increases with temperature and with increase in concentration of organic impurities and thickness of painted surfaces. The formation of methyl iodide has been confirmed through measurement of Total Organic Carbon (TOC) as shown in Fig. 7.5.4.

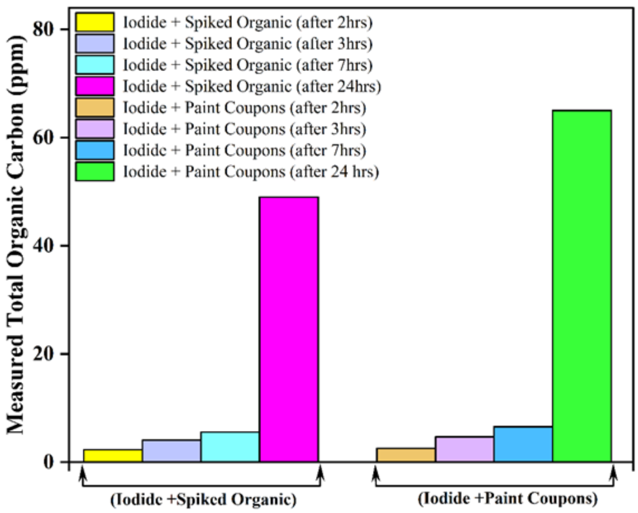

Fig.7.5.4: Measure TOC Values upon Interaction of Iodine with Painted Surfaces

The data generated through experiments would be very helpful in arriving at safety margins with regard to the iodine source term estimation, release inside the containment and planning the mitigation strategies to prevent iodine release to the environment.

7.5.5 Performance Evaluation of Alumina loaded Borophosphate Glasses for Waste Immobilization Applications

Borophosphate glasses have been explored as alternative matrices for waste immobilization applications owing to their superior characteristics over borosilicate counterparts. These glasses can be melted at lower temperatures thereby minimizing the volatilization of fission products during the vitrification process. Further, borophosphate glasses are known for their proven loading capacity for lanthanides and actinides, making them highly suitable for applications in waste immobilization. It is also observed that, addition of alumina to borophosphate glasses improves the overall structural and thermal properties of the matrices. In the present study, sodium calcium borophosphate glasses containing Al_2O_3 were synthesized using the conventional melt-quenching method. Structural characterization was performed using XRD, SEM-EDX and FTIR spectroscopic techniques to establish the suitability of the glasses. The analysis of the structural features indicated a uniform elemental distribution in the synthesized glasses. Studies on differential thermal analysis have demonstrated an enhancement in the thermal stability of borophosphate glasses, contributing to an increase in their chemical durability.

7.6 Reactor Physics Studies

7.6.1 Safety Assessment of Low Power Reactor Physics Experiments during 7th Fuel Cycle Operation of KKNPP-1

In the 7th fuel cycle of operation of KKNPP Unit-1, its fuel was partially switched from conventional UTVS to advanced TVS-2M type. To ensure that reactor physics parameters comply with the AERB safety criteria for such mixed core operation, independent verification calculations were carried out to support the safety review of the Low Power Physics Experiments at KKNPP Unit-1 during its Cycle-7 operation. These experiments were aimed to measure the temperature coefficient of reactivity, boric acid coefficient of reactivity, Emergency Protection (EP) worth, integral and differential worth of control groups of CPSARs etc. The measured values were compared with the theoretical estimations and found to be meeting the acceptance criteria.

7.6.2 Safety Review of the Proposal for Loading of RU/SEU Fuel Bundles in PHWR-220

It is envisaged to use Reprocessed Uranium (RU) in the currently operating 220 MWe PHWRs. The objective of using RU based fuel that could be slightly enriched uranium (SEU) is to enhance the average discharge burnup leading to reduced quantity of spent fuel generation during power operation. As a part of the safety review, verification of the reactor physics parameters was carried out by independent core physics analysis using DRAGON-DONJON code system, employing ENDF/B-VI.8 based cross-section data sets. The variation of neutron multiplication factors, isotopic composition changes with burnup, reactivity effects due to changes in moderator temperature, channel temperature, coolant temperature, fuel temperature, coolant void percentage, coolant/moderator purity, and boron/gadolinium poison concentration in the moderator etc. were calculated and found to be in good agreement with the design values.

7.6.3 Studies on the Neutronics Characteristics of VVER-1000 Reactor with Accident Tolerant Fuels

The neutronic characteristics of a VVER-1000 fuel assembly with Accident Tolerant Fuel (ATF), designed to endure severe accidents for a longer duration than the current UO_2/Zircaloy fuel were investigated. This work is taken up as an anticipatory R&D work. The analysis was carried out using the Monte Carlo based code, OpenMC with ENDF/B-VIII.0 based nuclear data. Both near-term concepts, such as, Cr-coated zircaloy claddings, Cr^{2O3}-doped UO_2 pellets, FeCrAl cladding and long-term concepts, such as, Uranium Nitride and Uranium Carbide (UC) fuel with SiC cladding, were considered for the analysis. Results of the study substituting ATF cladding for zircaloy, reveal a significant reactivity penalty for FeCrAl, a relatively smaller reactivity gain for SiC, and insignificant effects for Cr-coated cladding and Cr^{2O3}-doped pellets. Furthermore, for ATF fuels UN, UC, and Cr^{2O3} (1000 ppm) doped $UO_{2,}$ changes in reactivity and fuel isotopes were investigated and compared with conventional U^{O2} fuel. The variation of the infinite neutron multiplication factor ($K_{inf)}$ as a function of burnup is presented in Figs. 7.6.3(a) and 7.6.3(b) for various ATF cladding and fuel concepts, respectively.

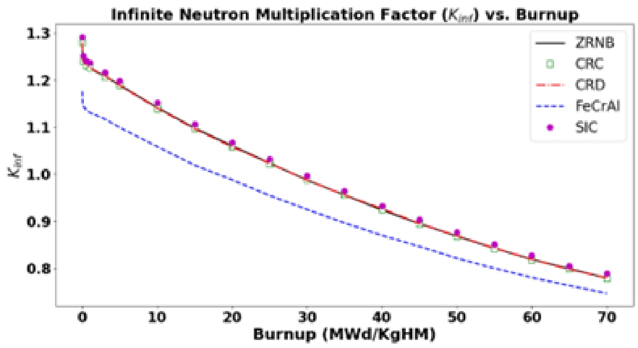

Fig.7.6.3(a): Variation of Neutron Multiplication Factor (K_{inf}) with Burnup

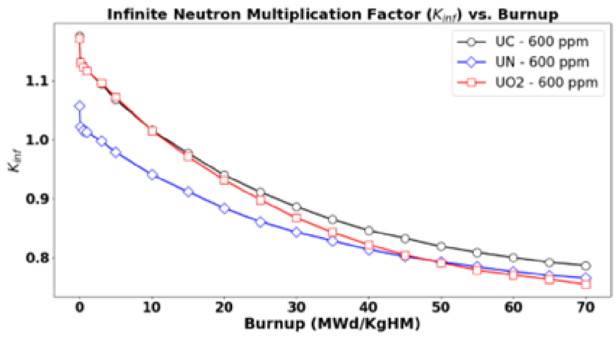

Fig.7.6.3(b): Variation of Neutron Multiplication Factor (K_{inf}) with Burnup

7.7 Structural Analysis and Material Studies

7.7.1 Development of Rolled joint model of Calandria tube in PHWR using ABAQUS

In PHWR, the calandria tube (CT) to calandria side tube sheet (CSTS) joint is a mechanical

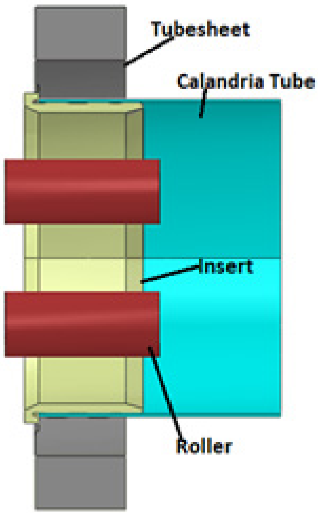

Fig. 7.7.1(a): Solid Model of the Rolled Joint Assembly.

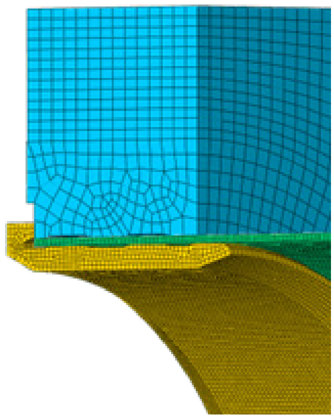

Fig. 7.7.1(b): Finite Element Discretization of the Rolled Joint Assembly

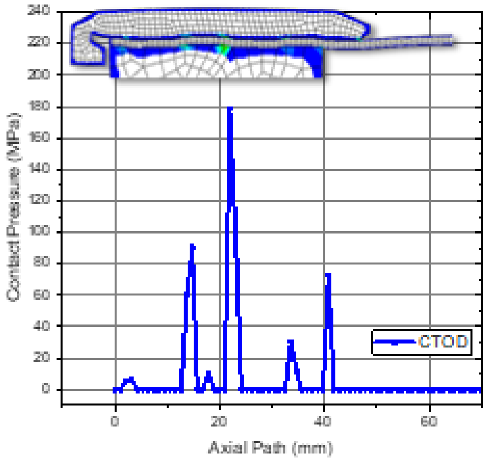

Fig. 7.7.1(c): Contact Pressure along Axis of Tube Developed at Calandria Tube Outer Surface

roller expansion joint. It is a special type of rolled joint called a sandwich rolled joint, wherein the calandria tube (Zircaloy-4) is sandwiched between the inner landed insert (made of SS 410 in full annealed condition) and the outer stainless steel tube sheet (SS 304L), as shown in Fig. 7.7.1(a). During the revision of safety guide on deterministic safety analysis of water cooled reactor based NPP (AERB/NPP-WCR/SG/D-19, Rev-1), acceptance criteria for calandria tube rolled joint temperature was deliberated. During anticipated operational occurrences (AOOs) and design basis accidents (DBAs), the temperature of CT-CSTS rolled joint will increase. It is important to maintain leak tightness and structural integrity of the rolled joint in these scenarios. Based on the deliberations in the meeting, assessment of the variation of contact pressure of the rolled joint with temperature is undertaken.

In the current work, the contact pressure after the formation of the joint at room temperature is evaluated. A 3D rolling simulation is carried out using ABAQUS as shown in Fig. 7.7.1(b). The analysis considers the motion of five rollers and the resulting plastic deformation. Finite element analysis shows that the contact pressure is not uniform along the axis of the rolled section and shows peaks at locations of local discontinuity due to grooves as shown in Fig. 7.7.1(c).

7.7.2 Structural Safety Assessment of Type C Package for Radioactive Material Transport

The safe transportation of relatively large amount of radioactive materials over long distances within short period will require Type C package. A type C package has to survive multiple stringent tests, the most notable being an impact test at a velocity not less than 90 m/s as per AERB Safety Code (AERB/NRF-TS/SC-1 (Rev.1)). The material must remain contained and shielded after the impact. Designing such packages is new, with limited tested concepts. A study has been initiated to explore energy absorption capabilities of such packages and proposes a new Type C package for a specific application.

In the present work, the dynamic deformation analysis of the PAT-2 package (Fig. 7.7.2(a)), designed by Sandia National Laboratory, USA is performed using ABAQUS/Explicit simulation. Weighing 33 kg and measuring 15 inches in diameter, the package was impacted at 90 m/s perpendicular to a rigid surface. The results

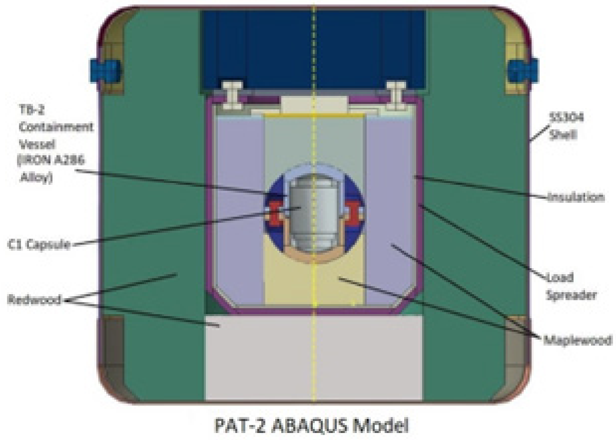

Fig. 7.7.2(a): PAT-2 Solid Model

indicate substantial deformation in both Redwood and Maplewood layers, while the inner containment vessel maintained integrity, securing radioactive materials (Fig. 7.7.2(b)). The study highlights the limitations of wood, specifically its impracticality for heavier packages due to low strength and large volume requirements.

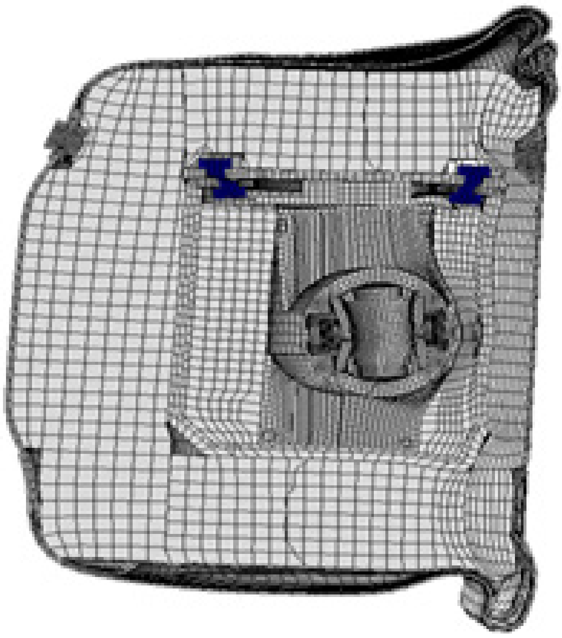

Fig. 7.7.2(b): Deformed Shape of PAT-2

Consequently, the usefulness of alternate energy absorbing materials, such as thin-walled metallic components, for heavier casks are being explored.

7.7.3 High Temperature Creep and Rupture Behaviour of Calandria Material SS 304L

Numerical studies associated with the structural integrity and retention capability of the calandria in the event of postulated severe accident scenarios in Pressurized Heavy Water Reactors (PHWRs) require high-temperature tensile and creep data of 304L SS. In this context, the behaviour of 304L stainless steel under high temperatures is analysed for creep deformation and rupture behaviour. Constant temperature and constant load uniaxial creep tests have been carried out at temperatures ranges from 973 K,1023 K and 1123 K, at selected stresses in the range of 250 MPa to 12.5 MPa.

It has been observed that both the secondary creep rate and rupture life follow a power-law dependence on the applied stress across all investigated temperatures (Fig. 7.7.3(a) and Fig. 7.7.3(b)). Particularly at 973 K, both the secondary creep rate and rupture life exhibited a two-slope

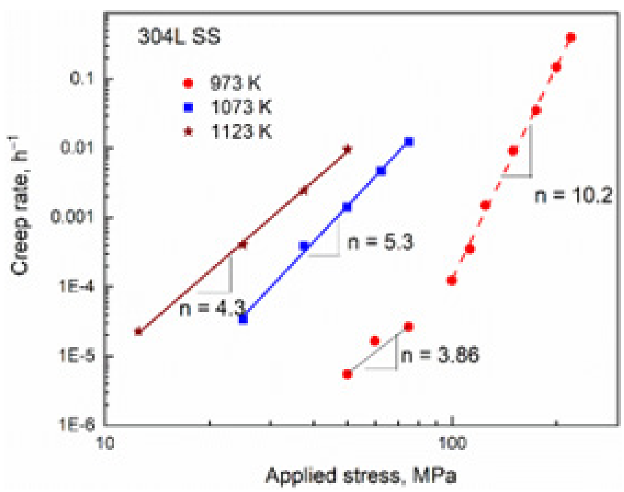

Fig. 7.7.3(a): Variation in Creep Rate versus Applied Stress

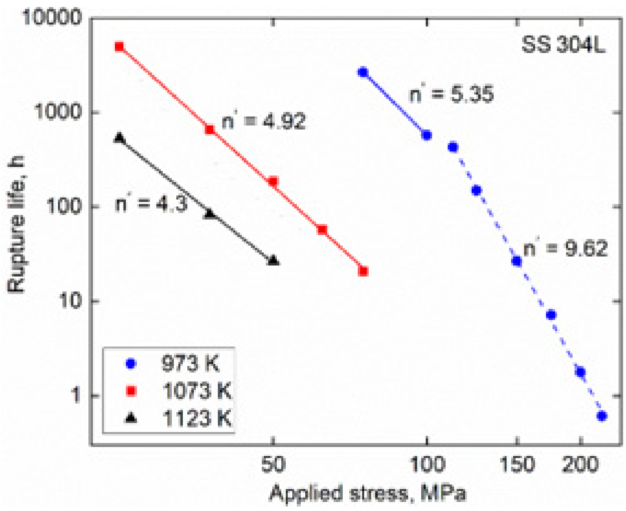

Fig. 7.7.3(b): Variation in Rupture Life versus Applied Stress

behaviour in relation to applied stress. The stress exponents associated with steady state (n) and rupture life (n) decrease with increase in temperature as well as with increase in applied stress. Further, a relation between applied stresses and Larson Miller parameter (LMP) was established, demonstrating the equivalence between rupture time and temperature. The Larson-Miller plot yielded a smooth master curve that facilitates prediction of stresses for any targeted exposure time and temperature within the investigated experimental domain. In addition to the above, creep rate evolution of 304L SS has been modelled by empirical models up to the onset of tertiary creep.

7.7.4 Deterministic Analysis of BWR Reactor Pressure Vessel using FAVOR Code

The Fracture Analysis of Vessels-Oak Ridge (FAVOR) computer program was developed by USNRC to perform deterministic and probabilistic risk-informed safety analyses of reactor pressure vessels (RPV) when subjected to a range of thermal hydraulic events. This code was used to perform deterministic safety assessment of the RPV of a typical BWR for flaws observed during in-service inspection (ISI). Different RPV load transients, like hydro test, normal start up and shutdown, upset, and emergency conditions were analysed. The results from thermo-mechanical analysis compared well with commercial FE software, ABAQUS. Typical hoop stress variation along RPV thickness is shown in Fig. 7.7.4(a) for the upset condition. Additionally, the stress intensity factors (SIF) for these flaws were also evaluated using FAVOR, which showed good agreement with SIF values obtained from in-house assessment

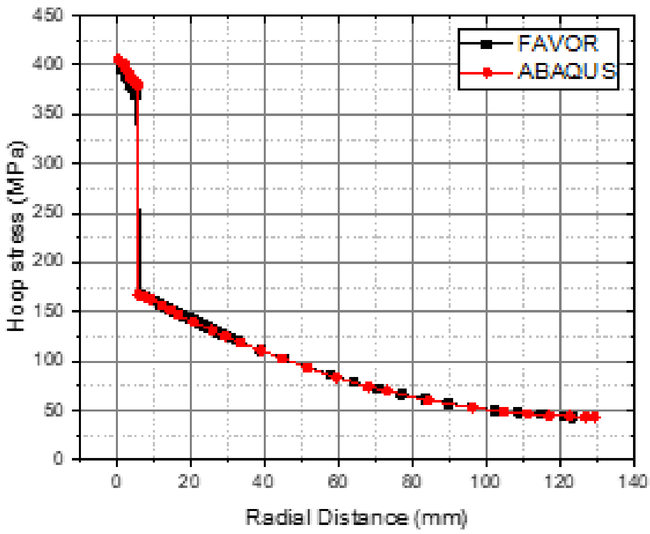

Fig. 7.7.4(a): Hoop Stress in RPV Wall

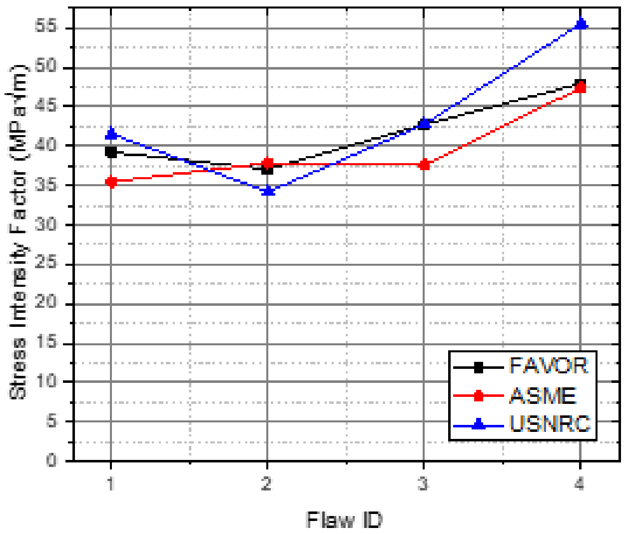

Fig. 7.7.4(b): SIF Values for Different Flaws

code based on ASME B&PV code and USNRC regulatory guide. The SIF values is illustrated in Fig. 7.7.4(b) for different surface flaws at the deepest point. Subsequently, FAVOR results were used for the deterministic safety assessment of RPV. Also, the benchmark problems with FAVOR is in progress to perform probabilistic safety assessment of RPV of LWRs.

7.8 Safety Studies to Support Review and Assessment

7.8.1 Study on Efficacy of Frequency Domain SSI Techniques for Deeply Embedded Structures

Seismic soil-structure interaction (Seismic SSI) plays a crucial role in structures that have large, deep foundations and embedment. Nuclear industry has largely relied on frequency domain approach as implemented SASSI software for Seismic SSI of safety related structures. Given the significance of Seismic SSI, a Standard Problem Exercise (SPE) was formulated in collaboration with the US NRC to evaluate the effectiveness of the frequency domain soil structural interaction method in analysing deeply embedded structures. The exercise involving simulation of responses of reactor turbine building configuration of NUPEC test was carried out for recorded ground motions in ACS SASSI software. The study reveals that the SSI methodology utilizing LB, BE, and UB soil characteristics effectively captures certain aspects of the dynamic behaviour of deeply embedded structures. However, some differences were observed in the frequency response spectra at high frequencies and induced pressure at deeper soil strata as shown in Fig. 7.8.1

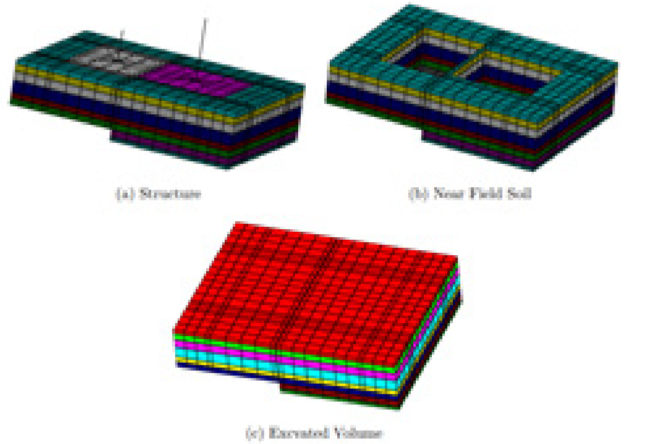

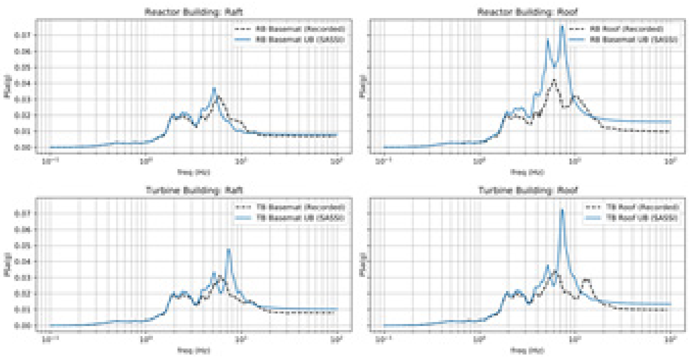

Fig. 7.8.1: Frequency Response Spectra at High Frequencies and Induced Pressure at Deeper Soil Strata

7.8.2 Safety Assessment of Primary Containment of 700MWe (KAPP-3&4) for Internal Pressure

During the review of analysis and design of containment structures, certain issues pertaining to analytical design model, such as eccentricity of unsymmetrical buttresses, unequal length of horizontal pre-stressing cable etc, were identified. It was decided to undertake a study on structural response of containment structure considering

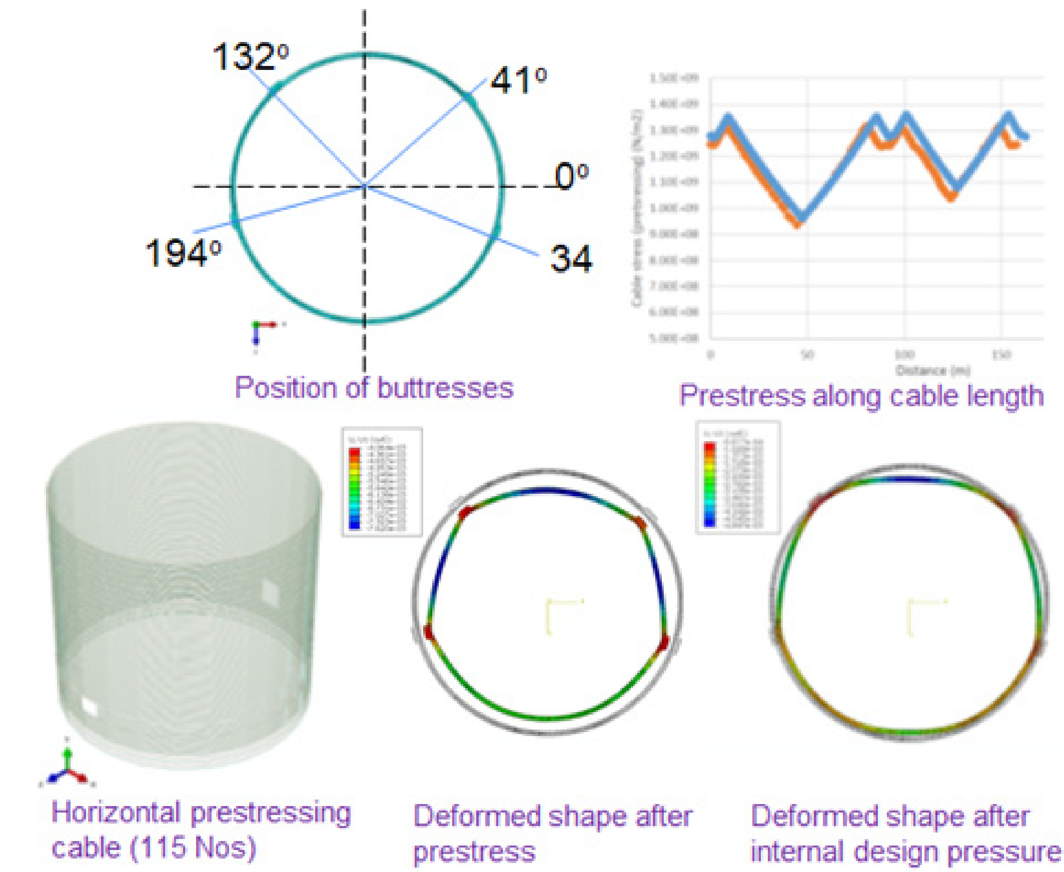

Fig. 7.8.2: Details of the Model and Results of Analysis

all aforesaid attributes. The study was divided into two phases; phase-1: structural response up to design limit and phase-2: structural response beyond design limit leading to ultimate load capacity (ULC).

Phase-1 of the study, where finite element model of containment structure is analyzed for internal pressure load up to design limit, was undertaken. The FE model considers detailed geometric features including individual pre-stressing cables considering elastic material properties. The analysis considered variation in pre-stress force along the length of the cable. Based on the analysis, deformations in IC wall as well as the dome are estimated immediately after pre-stress, after gravity and after application of pressure and compared with the undeformed state of the containment.

The deformation at the locations of buttress are seen to be lower compared to the deformations in the other areas due to eccentricity of the buttress from the IC centre line. The net deformation in West axis of IC wall at El 110m due to pressure loads is lower as compared to the East axis due to effect of additional stiffness near the MAL openings (Refer Fig.-7.8.2).

The study demonstrated the importance of modelling the pre-stressing buttress in the geometrical model and the variation of pre-stress along the length of cable to obtain the realistic responses of the containment structure.

7.9 AERB Funded Safety Research Programme

AERB promotes and funds research in radiation safety and industrial safety as part of its programme. AERB Committee for Safety Research Programmes (CSRP) frames guidelines for the same and also evaluates, recommends grants for research projects and monitor their progress periodically. During this period, CSRP approved renewal/extension of seven ongoing projects. The details are given in Table 7.1.

AERB also provides financial assistance to Universities, Research Institutions and Professional Associations for holding symposia and conferences on the subjects of interest to AERB. During this period, AERB had received about 28 applications requesting financial assistance for conducting Seminars, Symposium and Conferences.

Table 7.1: Research Projects Renewed/Extended

S. No.	Project Title	Principal Investigator	Organisation
1	Low Pressure Nanofiltration for Removal of Monovalent and Bivalent Salts from Leached Liquor during Alkaline Uranium Ore Processing	Prof. Sirshendu De	IIT, Kharagpur
2	Numerical Crack Growth Studies in Hydrided Pressure Tube of PHWR	Prof. Indra Veer Singh	IIT, Roorkee
3	Phytoremediation of Radioactive Elements (Cesium and Strontium) from Contaminated Soil and Water	Dr. N.K. Dhal	CSIR- IMMT Bhubaneswar
4	Experimental and Numerical Evaluation of Double Containment Structures of Indian PHWR against Hard Missile Impact due to External Event	Dr. Mohd. Ashraf Iqbal	IIT, Roorkee
5	Molten Corium Concrete Interaction Studies	Dr. Arunkumar Sridharan	IIT Bombay, Mumbai
6	Study of Fundamental Heat Transfer Characteristics in the Presence of Non-Condensable for Designing Long Term Passive Heat Removal System for Containment	Dr. Arunkumar Sridharan	IIT Bombay, Mumbai
7	Development of an On-Line Measurement System for Hydrogen Concentration in Steam Environment	Dr. U. Ramachandraiah	Hindustan Institute of Technology and Science, Chennai.